

TRANSVERSE BEAM PROFILE IMAGING OF FEW-MICROMETER BEAM SIZES BASED ON A SCINTILLATOR SCREEN

G. Kube, S. Bajt, DESY, Hamburg, Germany

A.P. Potylitsyn, L.G. Sukhikh, A.V. Vukolov, Tomsk Polytechnic University, Tomsk, Russia

I.A. Artyukov, P.N. Lebedev Physics Institute, Moscow, Russia

W. Lauth, Institut für Kernphysik, Mainz, Germany

Abstract

Standard beam profile measurements of high-brightness electron beams based on optical transition radiation (OTR) may be hampered by coherence effects induced by the microbunching instability which render a direct beam imaging impossible. As consequence, for modern linac based 4th generation light sources as the European XFEL which is currently under construction in Hamburg, transverse beam profile measurements are based on scintillating screen monitors. However, the resolution of a scintillator based monitor is limited due to intrinsic material properties and the observation geometry. In this report, a beam size measurement in the order of a few micrometer is presented using a LYSO scintillator, and discussed in view of the possible achievable resolution.

INTRODUCTION

Transverse beam profile diagnostics in electron linacs is widely based on optical transition radiation (OTR) as standard technique which is generated when a charged particle beam crosses the boundary between two media with different dielectric properties. Unfortunately, microbunching instabilities in high-brightness electron beams of modern linac-driven free-electron lasers (FELs) can lead to coherence effects in the emission of OTR, thus rendering it impossible to obtain a direct image of the particle beam. The observation of coherent OTR (COTR) has been reported by several facilities (see e.g. Ref. [1]), and in the meantime the effect of the microbunching instability is well understood [2]. In order to allow beam profile measurements in the presence of the instability, transition radiation based imaging in the EUV spectral region was successfully tested [3,4]. An alternative concept is to use scintillation screens because the emission of the scintillation light is a stochastic process from many atoms which is completely insensitive to the longitudinal bunch structure. A comprehensive overview over scintillating screen applications in particle beam diagnostics is given e.g. in Refs. [5, 6].

In a series of test measurements performed in the past few years, the applicability of inorganic scintillators for high resolution electron beam profile measurements was investigated [7, 8]. Most notably, the dependency of the resolution on the scintillator material and on the observation geometry was studied with respect to resolve beam profiles in the order of several tens of micrometers. Based on these measurements, high resolution screen monitor stations were designed for the European XFEL which is currently under

construction at DESY in Hamburg (Germany) [9]. Prototype monitors of this type are successfully in operation since about two years at the FLASH2 undulator beamline of the free-electron laser user facility FLASH at DESY [10]. These monitors use a 200 μm thick LYSO screen as scintillator.

The objective of the present study was to investigate the achievable resolution for micrometer beam sizes. For this purpose, scintillator based beam size measurements were performed at the 855 MeV beam of the Mainz Microtron MAMI (University of Mainz, Germany) which are presented in the following. Based on these measurements, the dependency of the beam size sensitivity on different experimental parameters was studied theoretically using a simple model to describe the scintillator influence.

EXPERIMENT AND DATA TAKING

The experiment was performed at the 855 MeV electron beam of MAMI with a beam current of about 250 pA. Fig. 1 shows a sketch of the experimental setup. The surface of

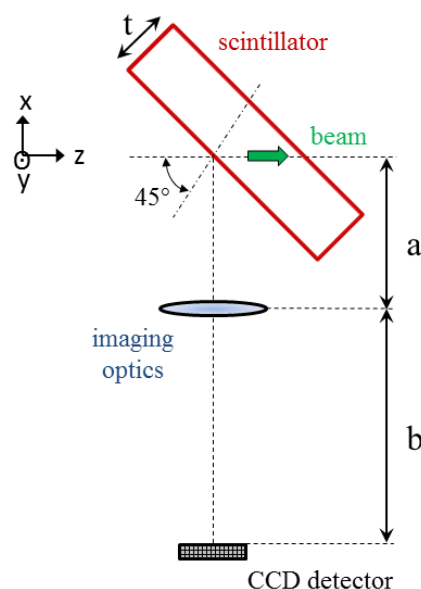


Figure 1: Sketch of the experimental setup (not to scale). The scintillator surface is rotated by 45 deg around the y -axis, observation is performed under 90 deg with respect to the beam axis.

a LYSO ($\text{Lu}_{2-x}\text{Y}_x\text{SiO}_5:\text{Ce}$) scintillator with thickness $t = 200 \mu\text{m}$ from the company *OmegaPiezo* [11] was tilted by 45 deg with respect to the beam axis, and observation was performed under 90 deg. The scintillating light generated by the electron beam inside the scintillator was imaged via an imaging optics onto a spatial resolving detector (CCD). As imaging optics, a Schwarzschild objective with nominal numerical aperture $\text{NA} = 0.19$ and focal length $f = 26.90 \text{ mm}$ was used which is described in detail in Ref. [12]. With an object distance $a = 27.54 \text{ mm}$ and an image distance $b = 1155.46 \text{ mm}$, the overall optical magnification of the system amounted to $M = 41.95$. The spatial resolving detector was a scientific grade CCD camera (ANDOR DO434 BN) with 1024×1024 pixels and a pixel size of $13 \times 13 \mu\text{m}^2$. For the measurements presented in the following, in vertical direction the range of interest was restricted to 275 pixels.

The scintillator measurements were performed in conjunction with an experiment to resolve sub-micron beam sizes based on OTR which required the chosen experimental geometry [4]. However, for resolution studies with a scintillator the 90 deg observation geometry is counteractive in the tilted horizontal (x -) plane because of the strong resolution broadening contribution, see Ref. [8]. Therefore, in the following only the vertical (y -) plane is considered for the resolution analysis.

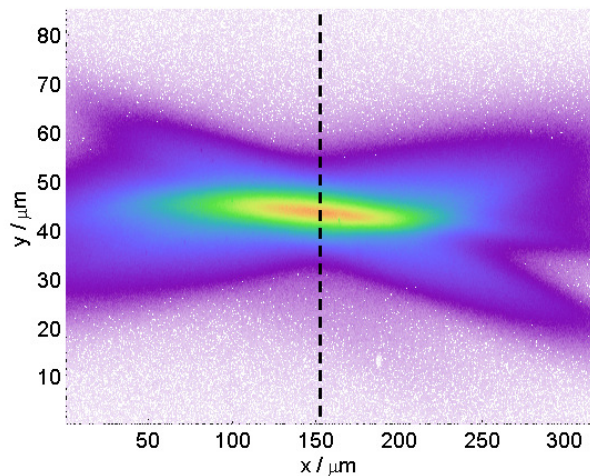


Figure 2: Beam image from LYSO scintillator, recorded with the CCD. The horizontal resp. vertical scales correspond to the object plane. The dashed line indicates the position onto the CCD chip which was used for the vertical profile analysis.

In Fig. 2 a beam spot measurement is shown which is the basis for the subsequent discussion. As can be seen, the beam image has a central core which resembles a Gaussian distribution, but it exhibits additional tails. These tails are caused by the scintillator, but also by the depth-of-focus effect of the optical system because the object plane (scintillator surface) was tilted versus the image plane (CCD chip). The horizontal position along the CCD at which the imaging condition is fulfilled is determined by the waist

in the vertical intensity distribution, cf. Fig. 2. This fact could simply be verified in the experiment by moving the Schwarzschild objective slightly along the optical axis, thus observing a horizontal shift of the waist onto the CCD.

ANALYSIS

In order to get rid of the depth-of-focus contribution, the analysis was performed only for that part onto the CCD for which the focusing condition is fulfilled. Therefore, in the following only the cut along the CCD column indicated by the dashed line in Fig. 2 is considered to represent the measured vertical beam distribution.

For the description of the scintillator properties and for the direct comparison with the experiment, the scintillator resolution was simulated using the optical ray-tracing program ZEMAX[®] [13], applying a simple model which was used earlier to describe the impact of the observation geometry [7, 8]. In this model, the scintillation light emission from a single electron is represented by a line source located inside the LYSO crystal which emits isotropically. The scintillator material properties are described by the wavelength dependent index of refraction, using a Sellmeier representation based on the data in Ref. [14]. The experimental setup in Fig. 1 is used as optical configuration, but for the sake of simplicity the imaging optics is described by a paraxial lens with the same focal length and NA than the Schwarzschild objective. For each configuration under investigation, in total 10^8 rays at a fixed emission wavelength (normally at the LYSO peak emission wavelength of 420 nm) are traced from inside the scintillator to the CCD, applying non-sequential ray-tracing. The resulting 2-dimensional intensity distribution is used as single particle resolution function (SPF), thus characterizing the scintillator influence. Finally, the resulting SPF is convolved with a 2-dim. Gaussian describing the electron beam profile, and the vertical cut through the maximum of this con-

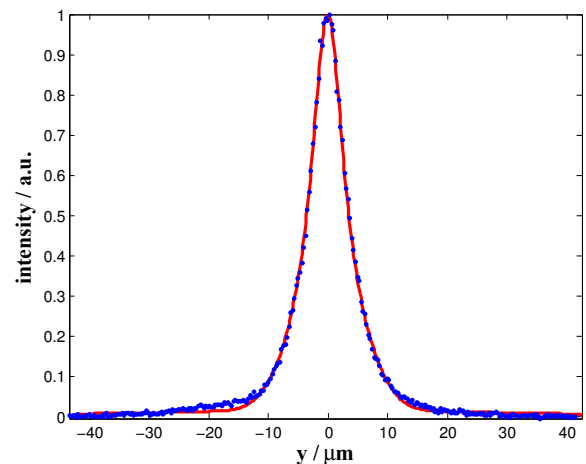


Figure 3: Comparison between measurement (blue dots) and simulation (red line). Both data sets were normalized to their maximum values. The calculation was performed for $\text{NA} = 0.20$ and a beam size of $\sigma_y = 1.44 \mu\text{m}$.

volution is compared with the cut along the experimentally recorded and background corrected CCD data as explained before. The agreement between simulation/convolution and the experimental data is evaluated based on a χ^2 calculation.

The comparison between the vertical beam profile measurement and the simulation shown in Fig. 3 suggests that the observed profile is described in a satisfactory way by means of the scintillator model described before. Moreover, the beam size of $\sigma_y = 1.44 \mu\text{m}$ used for the calculation indicates that it is possible to resolve transverse beam sizes down to the few micrometer level, perhaps even in the sub-micrometer range. The numerical aperture of $\text{NA} = 0.20$ for which the best agreement between measurement and simulation was achieved is slightly larger than the expected one of 0.19, which may be caused by the simplified description of the optical system by a paraxial lens. However, in the following the influence of some parameters is investigated and discussed in view of sensitivity for beam size determination.

Beam Size Fig. 4 shows a comparison between the measured beam profile and a simulated SPF which was convolved with different Gaussian distributions with beam sizes from 1-2 μm . As can be seen from this comparison, the difference in beam size is clearly visible, and the variation in the beam size affects the profile in the central part of the distribution. From this comparison it can be concluded that the sensitivity of the scintillator based beam size measurement is better than 1 μm .

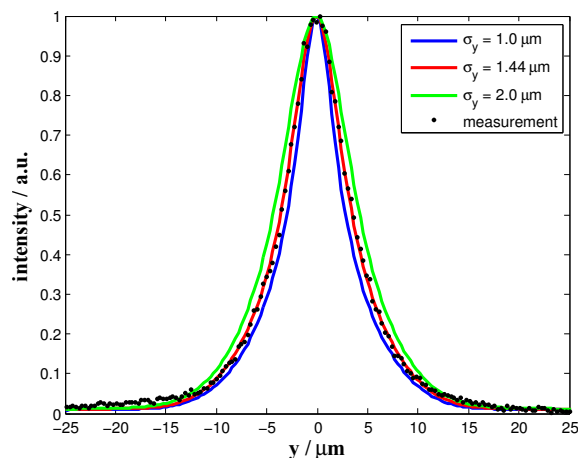


Figure 4: Comparison between measurement (black dots) and simulated SPF with subsequent convolution for three different vertical beam sizes (solid lines). The simulation was performed for $\text{NA} = 0.20$ at the LYSO peak emission wavelength $\lambda = 420 \text{ nm}$.

Numerical Aperture In the next step, SPFs were simulated for different numerical apertures and then convolved with beam distributions. Based on the χ^2 calculation, for each NA the vertical beam size was determined which resulted in the best agreement with the experimental data. As

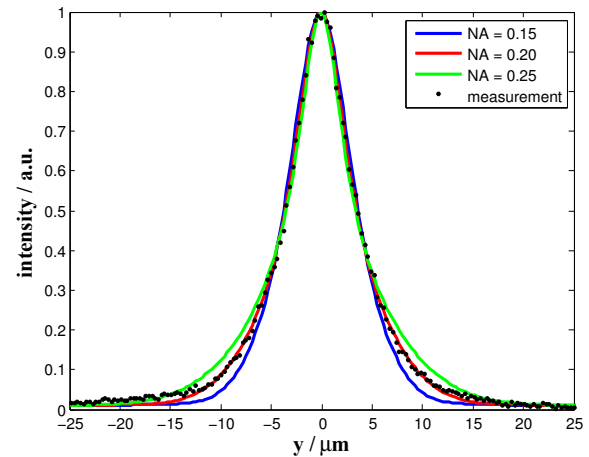


Figure 5: Comparison between measurement (black dots) and simulated SPFs for three different NAs (solid lines) with subsequent convolution. The simulations were performed for $\lambda = 420 \text{ nm}$.

an example, Fig. 5 shows a comparison for three different NA simulations. As can be seen from this figure, a difference in NA affects the profile in the tails of the distribution. Hence, variations in beam size and NA have different effects on the vertical beam distribution and can therefore be disentangled.

Fig. 6 summarizes the results of this investigation. As can be seen, with increasing NA the beam size decreases. This effect is probably caused by the minimization procedure: with increasing NA there is an increased contribution from the tails of the distribution, cf. Fig. 5, which is compensated by decreasing the beam size. However, as can be seen from the bottom of Fig. 6, there is a well defined parameter set $(\text{NA}, \sigma_y)_{opt}$ by which the measured distribution can be

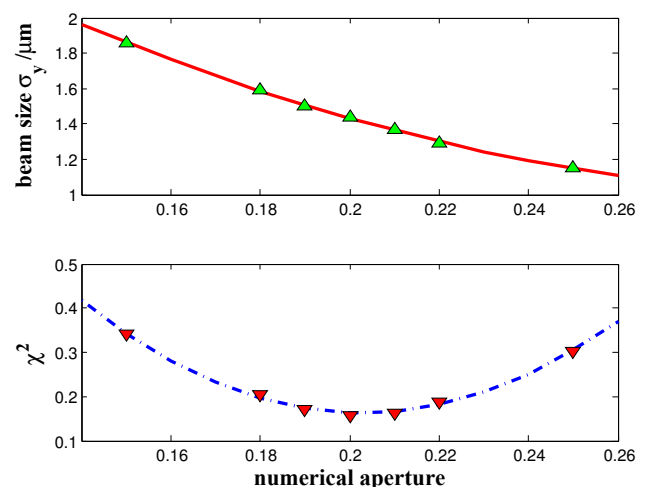


Figure 6: Top: Vertical beam size as function of the numerical aperture. The solid line shows a parabolic fit simply to guide the eyes. Bottom: The calculated χ^2 as function of NA indicates a well defined minimum.

characterized. As a conclusion, if there is an uncertainty in the numerical aperture it will be possible to determine both, beam size and aperture, from the experiment. At the other hand, according to Fig.6 the beam size variation required to compensate the uncertainty in NA is well below $1 \mu\text{m}$, i.e. the sensitivity of the scintillator based beam size measurement is still better than $1 \mu\text{m}$, even if the NA is not exactly known.

Wavelength As last point the dependency of the vertical beam size determination on the emission wavelength was investigated. LYSO has an emission spectrum from $\lambda = 350 \text{ nm}$ up to 620 nm with the peak emission at 420 nm . In the geometric ray-tracing model used to describe the scintillator properties, the wavelength dependency is introduced by the wavelength dependent index of refraction n which influences the refraction at the boundary between scintillator and vacuum. However, in the wavelength region from 360 nm up to 500 nm , where data for n were accessible [14], it decreases only slightly from $n(360\text{nm}) = 1.88$ down to $n(500\text{nm}) = 1.83$. Different SPFs were simulated for wavelengths between 400 nm and 500 nm , and the vertical beam size was deduced as described before. However, the variation in σ_y between $1.42 \mu\text{m}$ and $1.46 \mu\text{m}$ is negligible compared e.g. to the NA influence, therefore the wavelength dependency plays a minor role following the model simulations.

It should be noted that according to the manufacturer the LYSO refractive index at the peak emission wavelength amounts to $n(420\text{nm}) = 1.82$ [11] instead of 1.85 according to the Sellmeier parametrization [14]. However, due to the wavelength insensitivity this offset is negligible.

IMPROVEMENTS

Based on the model simulations described before, in this section possible improvements will be discussed which may help to increase the beam size sensitivity of a scintillator based profile measurement. In Fig. 7 the calculated vertical profile is shown for illustration together with the simulated SPF and the vertical electron beam profile. As can be seen from this comparison, the calculated profile is dominated by the SPF contribution. The best way to increase the beam size sensitivity is therefore to minimize this contribution.

A possibility to decrease the SPF contribution in vertical direction is to use a thinner scintillator. Fig. 8 shows simulated SPFs for different scintillator thicknesses and the same parameter set as before. As can be seen, for thinner scintillators the SPF contribution shrinks down and the beam size sensitivity increases. Going to much smaller thicknesses would even further reduce the SPF contribution, however from technical point of view the handling of a $50 \mu\text{m}$ thick scintillator is already difficult.

It is interesting to note that there is no significant difference between the SPF of a $200 \mu\text{m}$ and a $500 \mu\text{m}$ thick scintillator, in Fig. 8 they cannot be distinguished from each other. This observation can be interpreted such that from a

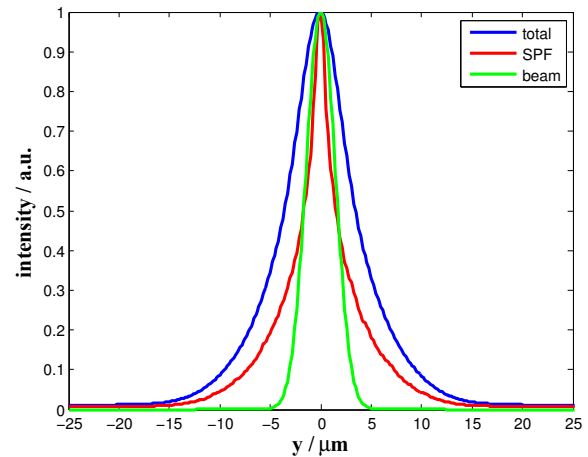


Figure 7: Contribution of the SPF (red curve) for $\text{NA} = 0.20$, $\lambda = 420 \text{ nm}$ and the vertical beam profile (green curve) for $\sigma_y = 1.44 \mu\text{m}$ to the best fit of the observed beam profile (blue curve).

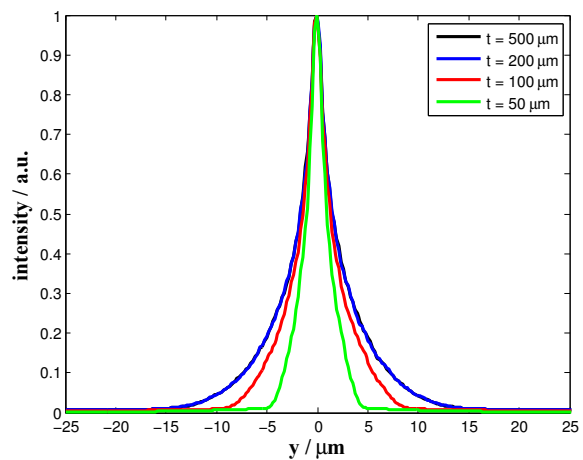


Figure 8: Simulated SPFs for different scintillator thicknesses. The simulations were performed for $\text{NA} = 0.20$ and $\lambda = 420 \text{ nm}$.

certain depth inside the scintillator, the radiation does not contribute significantly to the image formation, a point that has to be investigated more detailed in the future.

A further possibility to reduce the SPF is to change the observation geometry. As already mentioned in the introduction, the horizontal resolution is strongly affected by the observation geometry, and especially the 90 deg geometry used in this experiment is not optimal, see e.g. Refs. [7, 8]. In the vertical plane there exists additionally a dependence which is far less pronounced and which is beyond the scope of this investigation.

An important step towards a reliable high-resolution profile measurement can be achieved if the full 2-dim. information recorded by the CCD will be available for the analysis. In the present experiment the drawback was the depth-of-focus influence which allowed to use only a small region of the CCD. In order to correct perspective distortion

caused by the observation geometry over the whole CCD chip, the Scheimpflug principle can be applied, see e.g. Ref. [15]. This principle states that a planar object (scintillation screen) not being parallel to the image plane (CCD chip) will be completely in focus if the extended object-, lens- and image planes will intersect in one line, is already successfully applied for the screen monitors at the European XFEL [9]. In this case the SPF would correspond to the classical Point Spread Function (PSF), and the full 2-dim. beam profile could be reconstructed by classical deconvolution algorithms known from image processing, as for example the Lucy–Richardson algorithm [16].

SUMMARY AND DISCUSSION

In this report, a high resolution beam profile measurement based on a scintillating screen monitor is presented. Using a 200 μm thick LYSO:Ce screen it was possible to resolve a vertical beam size of $\sigma_y = 1.44 \mu\text{m}$. Based on a simple model to simulate the scintillator properties, the impact of different parameters on the sensitivity for beam size determination was investigated and improvements were pointed out.

However, care has to be taken specifying an absolute value for the beam size, the extracted value of 1.44 μm can be considered only as an upper limit. In this context one has to keep in mind that the resolution of a scintillator based profile measurement depends on the light generation and the light propagation. So far only the latter case was considered, i.e. the resolution contribution when the light produced inside the scintillator crystal has to reach the detector to contribute to the measurement, and for this it has to cross the boundary between scintillator and vacuum. But the light generation mechanism itself is a multi-stage process: according to Ref. [17], the sequence of processes leading to scintillation in a medium consists of 4 phases: (1) energy conversion, i.e. initial energy release with the formation of "hot" electrons and holes, (2) thermalization, i.e. the formation of electron-hole (e-h) pairs with an energy approximately equal to the band gap, (3) energy transfer to the luminescent centers, and (4) radiative relaxation of the excited centers. In Ref. [7] it was assumed that the first stage in this sequence dominates the resolution contribution, and the effect was estimated via the Fermi radius R_M for high-energetic electrons to be negligible. To estimate the contribution of the light generation process, an independent beam profile measurement is required which is not affected by this effect.

Such a measurement is available because the scintillator investigations presented here were performed in conjunction with an experiment to resolve sub-micron beam sizes based on OTR [4], and according to that experiment a beam size of $\sigma_y = 1.37 \mu\text{m}$ was deduced [18]. Under the assumption

that the discrepancy in both beam size measurements is caused by the light generation process inside the scintillator, this contribution can be estimated by subtracting both values quadratically, resulting in $\sigma_{res} = 0.44 \mu\text{m}$. This value can be considered to be an estimate for the fundamental resolution limit of a scintillator based profile measurement using a LYSO crystal. If a better resolution is required it will be necessary to find an appropriate scintillator material.

ACKNOWLEDGMENT

This work was partly supported by the by the Russian Ministry of Education and Science within the program "Nauka" Grant No. 3.709.2014/K.

REFERENCES

- [1] S. Wesch and B. Schmidt, Proc. DIPAC'11, Hamburg, Germany, May 2011, WEOA01, p.539 (2011).
- [2] G. Stupakov, Proc. IPAC'14, Dresden, Germany, June 2014, THYA01, p.2789 (2014).
- [3] L.G. Sukhikh, G. Kube, S. Bajt *et al.*, Phys. Rev. ST Accel. Beams **17** (2014) 112805.
- [4] L.G. Sukhikh, G. Kube, I.A. Artyukov *et al.*, these proceedings, TUPB011.
- [5] B. Walasek-Höhne and G. Kube, Proc. DIPAC'11, Hamburg, Germany, May 2011, WEOB01, p.553 (2011).
- [6] B. Walasek-Höhne *et al.*, IEEE Trans. Nucl. Sci. **59** (2012) 2307.
- [7] G. Kube, C. Behrens, W. Lauth, Proc. IPAC'10, Kyoto, Japan, May 2010, MOPD088, p.906 (2010).
- [8] G. Kube *et al.*, Proc. IPAC'12, New Orleans (Louisiana), USA, May 2012, WEOA02, p.2119 (2012).
- [9] Ch. Wiebers, M. Holz, G. Kube *et al.* Proc. IBIC'13, Oxford, UK, September 2013, WEPF03, p.807 (2013).
- [10] N. Baboi and D. Nölle, Proc. IBIC'14, Monterey (CA), USA, September 2014, THIXB1, p.712 (2014).
- [11] <http://omegapiezo.com/index.html>
- [12] I.A. Artyukov *et al.*, Opt. Commun. **102** (1993) 401.
- [13] <http://www.zemax.com>
- [14] M. Kronberger, PhD thesis, Technical University of Wien (2008), CERN-THESIS-2008-043.
- [15] H.M. Merklinger, *Focusing the View Camera*, Bedford, Nova Scotia: Seaboard Printing Limited (1996). <http://www.trenholm.org/hmmerk/download.html>
- [16] L.B. Lucy, Astronomical Journal **79** (1974) 745. W.H. Richardson, J. Opt. Soc. Am. **62** (1972) 55.
- [17] P. Lecoq *et al.*, *Inorganic Scintillators for Detector Systems*, (Springer Verlag, Berlin–Heidelberg, 2006).
- [18] L.G. Sukhikh, private communication (2015).